Accepted Manuscript

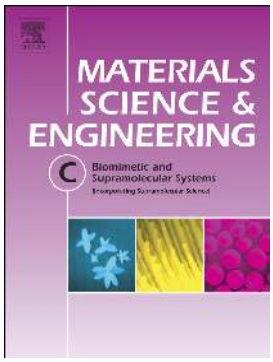

Development of 3D printable conductive hydrogel with crystallized PEDOT:PSS for neural tissue engineering

Dong Nyoung Heo, Se-Jun Lee, Raju Timsina, Xiangyun Qiu, Nathan J. Castro, Lijie Grace Zhang

PII: S0928-4931(18)32659-6
DOI: https://doi.org/10.1016/j.msec.2019.02.008
Reference: MSC 9401

To appear in: *Materials Science & Engineering C*

Received date: 24 September 2018
Revised date: 24 January 2019
Accepted date: 1 February 2019

Please cite this article as: D.N. Heo, S.-J. Lee, R. Timsina, et al., Development of 3D printable conductive hydrogel with crystallized PEDOT:PSS for neural tissue engineering, Materials Science & Engineering C, https://doi.org/10.1016/j.msec.2019.02.008

Development of 3D printable conductive hydrogel with crystallized PEDOT:PSS for neural tissue engineering

Dong Nyoung Heo,[a] Se-Jun Lee,[a] Raju Timsina,[b] Xiangyun Qiu,[b] Nathan J. Castro,[c] Lijie Grace Zhang,‡[a,d,e]

[a] *Department of Mechanical and Aerospace Engineering, The George Washington University, DC 20052, USA*

[b] *Department of Physics, The George Washington University, DC 20052, USA*

[c] *Institute of Health and Biomedical Innovation, Queensland University of Technology, Queensland, Australia 4059*

[d] *Department of Biomedical Engineering, The George Washington University, DC 20052, USA*

[e] *Department of Medicine, The George Washington University, DC 20052, USA*

* Correspondence to Lijie Grace Zhang, Ph. D.

Department of Mechanical and Aerospace Engineering,

The George Washington University,

3590 Science and Engineering Hall, 800 22nd street, NW, DC 20052, USA

Tel.: 1-202-994-2479

E-mail address: lgzhang@gwu.edu (Lijie Grace Zhang).

Abstract

Bioelectronic devices enable efficient and effective communication between medical devices and human tissue in order to directly treat patients with various neurological disorders. Due to the mechanical similarity to human tissue, hydrogel-based electronic devices are considered to be promising for biological signal recording and stimulation of living tissues. Here, we report the first three-dimensionally (3D) printable conductive hydrogel that can be photocrosslinked while retaining high electrical conductivity. In addition, we prepared dorsal root ganglion (DRG) cell-encapsulated gelatin methacryloyl (GelMA) hydrogels which were integrated with the 3D printed conductive structure and evaluated for efficiency neural differentiation under electrical stimulation (ES). For enhanced electrical conductivity, a poly(3,4-ethylenedioxythiophene) (PEDOT): polystyrene sulfonate (PSS) aqueous solution was freeze-dried and mixed with polyethylene glycol diacrylate (PEGDA) as the photocurable polymer base. Next, the conductive hydrogel was patterned on the substrate by using a table-top stereolithography (SLA) 3D printer. The fabricated hydrogel was characterized for electrochemical conductivity. After printing with the PEDOT:PSS conductive solution, the patterned hydrogel exhibited decreased printing diameters with increasing of PEDOT:PSS concentration. Also, the resultant conductive hydrogel had significantly increased electrochemical properties with increasing PEDOT:PSS concentration. The 3D printed conductive hydrogel provides excellent structural support to systematically transfer the ES towards encapsulated DRG cells for enhanced neuronal differentiation. The results from this study indicate that the conductive hydrogel can be useful as a 3D printing material for electrical applications.

Keywords: 3D printing, electrical stimulation, neurogenic differentiation, photocurable hydrogel, conductive polymer

1. Introduction

Electrical stimulation (ES) has been employed as a means to understand and modulate fundamental biological processes including cell division, orientation, migration, differentiation, extracellular matrix deposition and cytokine release [1, 2]. Additionally, ES can be used to enhance the neural differentiation from incorporated stem cell and provide the neural signal connection with cell-cell interaction [3-5]. For this reason, many studies have dedicated significant effort to develop biocompatible materials capable of conducting ES [6-9].

Conductive polymeric materials provide an invaluable tool for the fabrication of an electrically conductive substrate to directly interface between scaffolds and electro-active tissues [10-12]. In addition, electrically conductive polymers can enhance the composite biomaterial-tissue interface and modulate desired cell responses such as proliferation and differentiation [13-17]. Therefore, the use of electrically active conductive polymers extends the functionality of biomaterials through the incorporation of ES rendering them more effective for various biomedical applications including bimodal neural probes, tissue engineering, spinal cord repair, artificial muscles, sensing devices, and drug delivery system [18, 19].

Although conductive polymeric materials have intriguing properties suitable for various electronic applications which interface with living tissue, they have a few drawbacks that must be mitigated. Since all conductive polymeric materials have poor solubility and are mechanically brittle due to the rigid pi-bonding, they have a limitation on the practical implementation and structure formation in clinically useful devices or engineered tissues [20-22]. Therefore, we focused on the design, development, and evaluation of a patternable conductive hydrogel by 3D printing. Amongst the various investigated conductive polymeric materials, poly(3,4-ethylenedioxythiophene) (PEDOT): polystyrene sulfonate (PSS) has been

shown to be the most useful polymeric material for biomedical applications because of its excellent chemical stability, electrical properties, and biocompatibility [23-25]. Therefore, we expect PEDOT:PSS to be a suitable choice of base biomaterial for 3D printable conductive hydrogel. 3D printing conductive hydrogels are useful for the development of a new generation of biomedical devices requiring ES.

In this study, we developed a photocrosslinkable conductive hydrogel containing various concentrations of PEDOT:PSS, which provides a highly electrochemical environment. Next, we optimized 3D printing conditions for the fabrication of 3D structures with optimal conductivity and geometrical design. As a proof-of-concept study illustrating the effectiveness of the fabricated 3D conductive structure and ES, encapsulated dorsal root ganglion (DRG) neuronal cells were stimulated and evaluated for neuronal differentiation.

2. Experiment Section

2.1 Fabrication of photocurable conductive hydrogel

The 3D printable conductive hydrogel was prepared based on a previously reported method [25, 26]. To obtain the PEDOT:PSS solid, the as-received PEDOT:PSS aqueous solution (Clevios P, Heraeus) was placed in a deep freezer (-80 °C) for 1 day, and lyophilized for 3 days. The fully dried PEDOT:PSS solid was dissolved in 7 ml of a mixed solution with distilled water (DW) and ethylene glycol (EG) (8:1) with various weights of 35, 49, 70, and 91 mg. For photocrosslinking, 3ml of polyethylene glycol diacrylate (PEGDA) containing 0.5 wt% photo-initiator [bis(2,4,6-trimethylbenzoyl)-phenylphosphineoxide (BAPO) (BASF, Florham Park, NJ)] was added to obtain a 30 wt% solution. Subsequently, the mixture was poured on a glass slide with a spacer of 1 mm thickness, and photocrosslinked via ultraviolet (UV) exposure for 60 sec. To remove the extra ions and impurities, all hydrogel samples were washed 3 times for 5 min in DW and placed in DW overnight before characterization.

2.2 3D photo-patterned conducting hydrogel design and fabrication

The 3D photo-patterned conductive hydrogels were designed and printed based on our previously reported method. [27] For patterning the conductive hydrogel, the computer-aided design (CAD) based architectural models with square pores were designed with various fiber spacing of 500, 600 and 800 μm. Next, the 3D structure was printed using a Solidoodle® 3D printer platform with X-Y-Z controlled UV laser system. The conductive printing solutions composed of PEGDA, PEDOT:PSS and photoinitiator were placed on the Z-controlled movable container and printed by UV laser exposure. The printing parameters were as follows: 200 μm diameter laser spot, 355 nm wavelength of UV parameter, 20 μJ intensity at 15 kHz of energy output, and 8 mm/sec printing speed.

2.3 Characterization of the fabricated conductive hydrogel

After fabrication of photocrosslinked conductive hydrogels, optical images were acquired by

optical microscopy (Mu800, AmScope) and converted to a 3D surface plot by image analysis software. Acquired optical images were used to calculate the average diameter of the 3D printed hydrogel by ImageJ (NIH Freeware). To characterize the mechanical properties of each hydrogel sample, an 8 mm x 2mm (diameter x thickness) was measured by an MTS criterion universal testing system (MTS Corporation, USA) in single uniaxial compression mode (n = 6) and their strain-stress relationship. The static compression force was applied at a rate of 5 mm min^{-1}, and results were plotted as a stress-strain curve.

To investigate the electrochemical properties, the conductive hydrogels were cut into a cylindrical shape (10 mm in diameter and 1 mm in height) using a biopsy punch and characterized by cyclic voltammetry (CV) and sheet resistance measurement. CV measurement was performed using a multichannel potentiostat (DY2013, Digi-Ivy, Inc., TX, USA) with a standard three-electrode system, which consists of a working electrode, a platinum counter electrode, and an Ag/AgCl reference electrode. The conductive hydrogel constructs were attached to an electrical lead and used as working electrodes. The CV curves were obtained after 5 repetitive potential scans in the range of -0.8 V to 0.8 V at a scan rate of 100 mV/s. The sheet resistance was measured using a four-point sheet resistance meter (RC2175, EDTM).

Fourier transform infrared (FTIR) spectra were recorded with the sample/potassium bromide (KBr) pressed pellets using a PerkinElmer Spectrum 100 FTIR spectrometer. X-ray diffraction (XRD) measurements were carried out at room temperature with an in-house x-ray scattering instrument. The x-ray beam is generated by a Genix3D integrated micro-focus fixed anode (Copper) source operated at 30 kV and 0.28 mA. Two sets of scatter-less slits are used to collimate the beam to a size of 8x8 mm at the sample. The x-ray exposure time was 60 minutes, and scattering intensities were registered by a mar345 image plate detector at around 20 cm distance from the sample. The data were analyzed using home-written Matlab

codes.

2.4 Neuronal cell proliferation and viability assay

Immortalized dorsal root ganglion (DRG) neuronal cell lines (50B11, provided by Dr. Ahmet Hoke) were used for all cell studies. DRG cells were cultured in T-75 flasks with Neurobasal medium composed of 10% fetal bovine serum (FBS), 0.2% glucose, 0.5 mM glutamine, B-27 supplement, and maintained in standard cell culture.

For biological experiments, the conductive hydrogels were cut into cylindrical shape using a 10 mm biopsy punch and placed in 12-well culture plates. DRG cells were harvested and seeded on the surface of conductive hydrogels at a cell density of 5×10^4 cells in 200 µl medium. After allowing for cell attachment (4 h), the fresh culture medium was carefully added in the culture plates. Cell proliferation on the hydrogel surface was quantified after 24, 48, and 72 h by using a cell counting kit (CCK-8, Dojindo Dojindo Molecular Technologies Inc., Japan). At different incubation time points, fresh medium containing CCK-8 was added in the culture plate, incubated for 2 h, and measured their absorbance at 450 nm by using a Multiskan GO microplate spectrophotometer (Thermo Fisher Scientific, USA). Additionally, the cell viability was confirmed by using a live/dead assay kit (Invitrogen, USA) after 24 h of incubation. The cell-seeded hydrogel samples were rinsed with Dulbecco's phosphate buffered saline (DPBS) and treated with the solutions of 2 mM calcein AM and 4 mM EthD-1. Then, the stained cells were observed and imaged using a Zeiss 710 confocal laser scanning microscopy.

2.5 Cell encapsulation in GelMA hydrogel incorporated 3D photo-patterned conducting hydrogel structure

To prepare the encapsulated DRG cells which were placed in the pores of the conductive hydrogel structure, gelatin methacryloyl (GelMA) was synthesized using gelatin derived from type A porcine skin and functionalized as previously described. [28] Synthesized GelMA was

utilized for cell encapsulation. Hydrogel precursor containing 7 wt% GelMA and 0.1 wt% photoinitiator was dissolved in DPBS, and mixed with DRG cells to create a cell density of 2 × 10^6 cells mL^{-1}. Further, 200 µl of the hydrogel-cell mixture was carefully dispensed in the conductive hydrogel structure and crosslinked by exposure to UV for 60 sec. After encapsulating the cells, the crosslinked hydrogel constructs were cultured in standard cell culture medium condition for evaluating the cell viability study. To evaluate the effect of the conductive hydrogel structure with electrical stimulation (ES) on neurogenic differentiation, cell-laden hydrogel structures were cultured in Neurogenic differentiation medium (C-28015, PromoCell, UK). After then, ES was applied with two parallel stainless steel electrodes that place on two ends of each custom-made well plate cover. The cell-laden hydrogel structures were placed at the center of the two electrodes and the ES was applied with 1000 mV/sample of the steady state direct current (DC) electric field for 2 days.

2.6 Immunofluorescence staining analysis

In order to confirm that the encapsulated DRG cells inside the conductive hydrogel structure induce neural differentiation via ES, immunofluorescent staining was performed with specific antibodies to visualize the neurogenic gene expression. The samples were fixed in 10% formalin for 60 min, permeabilized in 0.1% Triton X-100 for 30 min, and incubated with 2.5% bovine serum albumin (BAS) for 60 min to block nonspecific background staining. The samples were incubated with a polyclonal rabbit anti-neurofilament heavy polypeptide (Abcam) and a monoclonal mouse anti-Tubulin β 3 (BioLegend) overnight at 4ºC. Samples were washed three times with DPBS and subsequently incubated with the secondary antibody (Alexa Fluor 488 or 594 antibodies, Invitrogen) for 1h at room temperature. After three washing with DPBS, the samples were counterstained with DAPI, and taken the images using confocal microscopy.

2.7 Quantitative real-time polymerase chain reaction (qPCR)

To evaluate the neurogenic gene expression levels of BDNF, NT-3, and erbB2, real-time PCR was performed after 2 days of neurogenic differentiation culture. The isolation of total RNA from the encapsulated DRG cells cultured with and without ES was performed using an RNeasy Plus Mini Kit (Qiagen, USA). qPCR reaction was performed as previously described [29], using the following primers: for BDNF: 5´-CAA AAG GCC AAC TGA AGC-3´ (sense); 5´-CGC CAG CCA ATT CTC TTT-3´ (anti-sense); for NT-3: 5´-AAC GAG GTG TAA AGA AGC-3´ (sense); 5´-TGT CTA TTC GTA TCC AGC-3´ (anti-sense); for erbB2: 5´-TGA CAA GCG CTG TCT GCC G-3´ (sense); 5´-CTT GTA GTG GGC GCA GGC TG-3´ (anti-sense).

2.8 Statistical analysis

All values were presented as the mean ± standard deviation (SD). A one-way analysis of variance (ANOVA) with Dunnett's T3 post-hoc paired comparison test was used to verify statistically differences among groups, and the results were presented as the mean ± standard deviation (SD). The differences with p-values (p<0.05) were considered statistically significant.

3. Results and Discussion

3.1 Fabrication of 3D photo-patterned conductive hydrogel structure

A schematic diagram of the overall fabrication process of the 3D conductive hydrogel structure is shown in **Figure 1**. In this study, we used a stereolithography (SLA) 3D printing system to pattern the conductive hydrogel with pre-designed architecture. First, 3D printable conductive hydrogels were prepared with various PEDOT/PSS concentration from 0.00% to 0.91%, and characterized for printability. After photocrosslinking the hydrogels, optical transparency decreased with increasing PEDOT/PSS concentration (**Figure 2A**). It is due to the presence of PEDOT/PSS in the hydrogel structure. In contrast, the hydrogel without PEDOT/PSS was almost transparent. After 3D printing of PEDOT/PSS hydrogel, the resulting hydrogel diameters were decreased from 401.1 ± 52.8 μm to 284.7 ± 16.2 μm with increased PEDOT/PSS concentration, respectively (**Figure 2B, C**). In the case of the hydrogel without PEDOT/PSS, the resultant hydrogel did not exhibit the pre-designed open pore geometry as shown in 3D surface plot images which may be due to the low printing resolution caused by the diffusion of UV light [30]. Therefore, we could not measure the resulting hydrogel diameter for the hydrogel without PEDOT/PSS.

3.2 Mechanical properties of the photocurable conductive hydrogel

Prior to patterning the conductive hydrogels, their mechanical properties were measured using a universal compression testing machine. The compressive stress-strain curves showed an increase in strain with increasing PEDOT/PSS concentration (**Figure 3A**). The compressive stiffness decreased from 35.4 ± 1.4 MPa to 26.3 ± 4.2 MPa with increased PEDOT/PSS concentration (**Figure 3B**). It is because of penetrated UV light intensity into the PEDOT/PSS photo-curable solution. As shown in Figure 2A, penetrated UV light through cross-linked hydrogel was decreased with increased PEDOT:PSS concentration. Therefore, the crosslinking efficiency of PEDOT/PSS hydrogels decreased with increasing PEDOT/PSS

concentration since the addition of PEDOT/PSS in the hydrogel lead of a decrease in transparency [31, 32]. In terms of mechanical properties, a previous report described that PEDOT/PSS hydrogel had a compression stiffness of 1.6 kPa [33]. In comparison with our results, the photocurable conductive hydrogel composed of PEDGA and PEDOT/PSS exhibited a much higher compression stiffness in the range of 26.3–35.4 MPa than that (1.6 kPa) of PEDOT/PSS hydrogel. It is due to the main composition of the stiffer PEGDA polymer network into the conductive hydrogel matrix. Although the mechanical properties of PEDOT/PSS hydrogels decreased when compared to pure hydrogel control, the structural integrity of the resultant 3D printed construct was retained during the printing process.

3.3 Chemical characterization of photocurable conductive hydrogel

1H NMR spectroscopy was employed to demonstrate successful synthesis of GelMA. The new peaks at 5.3 and 5.6 ppm in the GelMA spectra, when compared to the gelatin powder spectrum, are assigned to the protons of the MA residues (**Supplementary figure S1**). These residues occur during GelMA synthesis via amide reaction by modifying methacrylate on the amino group of gelatins.

Similarly, we performed FTIR to determine the chemical structure of fabricated hydrogel structures as well as gelatin and GelMA. In the case of pristine gelatin, the C=O stretching vibration appearing at 1660 cm^{-1} demonstrated the amide I band, while the amide band II indicating the N-H bending vibration was observed at 1535 cm^{-1} (**Supplementary figure S2A**). A typical hydroxyl group peak of GelMA was observed at around 3252 cm^{-1}. GelMa showed all the characteristic peaks of gelatin such as those at 1640 cm^{-1} and 1545 cm^{-1}, which indicated the successful reaction between gelatin and methacrylate. Additionally, the characteristic bands for gelatin functionalized methacrylate at 1440 cm^{-1} (amide III), corresponding to the bending of N-H bond and plane vibration of N_H were observed. The FTIR spectrum of PEGDA, as seen in supplementary figure S2B shows a peak at 1730 cm^{-1},

attributed to C=O symmetric stretching and at around 1640 cm^{-1}, attributed to C=C stretching arising from the presence of terminal acrylate group. Additionally, -OH bond was found at around 3500 cm^{-1}. The FTIR spectrum of PEDOT/PSS hydrogel shows a peak at 1145 cm^{-1}, which is assigned to the stretching modes of the ethylendixoy group. Peaks at around 1200 cm^{-1} are corresponding to the sulfone groups in the molecules of PSS. (**Supplementary figure S2B**).

The XRD patterns of Gelatin and GelMa are shown in supplementary figure S3A and XRD patterns of PEDGA, PEDOT/PSS, and PEDOT/PSS hydrogel are shown in the figure S3B. The peak at Q value around 1.18 $Å^{-1}$ (2θ around 16^{o}-17^{o}) for all the samples are due to the Mylar window. The weak peak at Q value around 1.78 $Å^{-1}$ (2θ around 25^{o}-26^{o}) is from the background. The absence of pronounced XRD peaks for PEDOT/PSS, Gelatin and GelMa indicate that these are amorphous at room temperature. The very broad peak for PEGDA at Q value around 1.6 $Å^{-1}$ (2θ around 22^{o}-23^{o}) indicates that PEGDA is relatively ordered compared with PEDOT/PSS, Gelatin and GelMa. For PEDOT/PSS hydrogel, at Q value around 1.5 $Å^{-1}$ (2θ around 22^{o}-23^{o}), there exists a peak which is sharper than the peak for PEGDA, which suggests that PEDOT/PSS hydrogel is most ordered sample between these 5 samples.

3.4 Electrochemical properties of the photocurable conductive hydrogel

The electrical properties of the conductive hydrogels were evaluated by comparing CV and sheet resistance with different PEDOT/PSS concentration. As shown in **Figure 4A**, the CV results showed different charge delivery capacity (CDC) evident by the area within the cyclic graph. The CDC of the conductive hydrogel significantly increased as a function of PEDOT/PSS concentration which may be attributable to an enlarged electrical activation area caused by PEDOT/PSS. In addition, the presence of ethylene glycol (EG) in the 3D printing solution contributed to the CDC of conductive hydrogels. The CDC of PEDOT/PSS hydrogel

with EG was higher than that without EG (**Figure 4B**). Previous reports described that the addition of EG induced a significant structural rearrangement of PEDOT/PSS towards the formation of crystallized nanofibrils form, and improved its conductivity by the nanofibril-based network of the PESOT/PSS phase [34, 35]. In addition, the electric sheet resistance was observed to significantly decrease with increasing PEDOT/PSS concentration (**Figure 4C**). Interestingly, the sheet resistance of 0.91 % PEDOT/PSS hydrogel without EG significantly increased from 662.0 ± 100.6 Ω/sq to 968.0 ± 245.1 Ω/sq when compared to samples containing EG. As noted earlier, the enhanced electrical properties of CV and sheet resistance are due to the realignment of densely packed and highly ordered PEDOT/PSS structure [36].

3.5 Cell viability on the conductive hydrogel surface

To evaluate the cytotoxicity of the conductive hydrogel surfaces, DRG cells were cultured upon hydrogels with various PEDOT/PSS concentrations and evaluated for viability by using the CCK-8 assay at 24, 48 and 72 h. It was found that no cytotoxic effect was observed from these surfaces up to 72 h (**Figure 5A**). Cell proliferation of all of the groups slightly increased throughout the cell culture period. The presence of PEDOT/PSS exhibited a slight positive effect on cellular behavior where cell number increased with the addition of PEDOT/PSS into the hydrogel. Also, we confirmed cell cytotoxicity of the conductive hydrogel with various concentration of PEDOT/PSS by live/dead staining and confocal laser scanning microscopy. Confocal images revealed considerable DRG viability (**Figure 5B**). In addition, the number of living cells significantly increased with increasing concentration of PEDOT/PSS. These results indicate that the addition of PEDOT/PSS into PEG hydrogels induces a positive influence on the cell adhesion and proliferation. It is well known and recognized that PEG has unique properties to inhibit non-specific protein adsorption. However, the combination of PEG hydrogels with crystalline polymers, nano- or

microparticles, and nano- or microfibers has led to further enhanced cell behavior of numerous cell types [27, 37]. Similarly, a recent study by Yang et al. revealed that incorporation of a conductive polymer such as PPY into hydrogel enhance hMSC adhesion, suggesting that conducive polymer doped with anions can support cell adhesion and growth of various cells [16]. In this study, the PEDOT/PSS into the PEG hydrogel existed in the aggregation of PEDOT/PSS structures. For this reason, the addition of PEDOT/PSS polymers could give the conductive hydrogel many advantages such as high affinity for cell attachment and proliferation than non-conductive PEG hydrogel.

3.6 Design and fabrication of 3D-printed conductive hydrogel structures with a varied pore distribution

3D-printed conductive hydrogels were fabricated via a SL-based 3D printer using PEDOT:PSS hydrogel solution. **Figure 6A** illustrates the computer-aided design (CAD) architecture with dimensions of 12 mm x 0.8 mm solid squares with square pore geometry. 3D-printed conductive hydrogels with increasing in-fill density (a distance of patterned line: 0.5, 0.6, and 0.8 mm) were printed for embedding of live cells. Optical images illustrate that the resultant hydrogel structures had parallel-aligned fibers with orthogonal orientation. In an effort to verify the influence of 3D-printed conductive hydrogels on cell viability and cytotoxicity, DRGs were encapsulated within a gelatin-based hydrogel and subsequently embedded in the 3D structure and evaluated via live/dead assay (**Figure 6B**). Confocal microscopic images showed that most encapsulated DRGs retained their viability after 1 day of culture. Also, all of 3D printed structure with varying pore size, excellent cell viability with horizontal and vertical orthogonal lines producing a square pore geometry. These results indicate that the conductive hydrogel has no significant cytotoxicity toward DRGs. Additionally, an image of the letters “BIO ELECTRODE” were successfully printed using conductive hydrogels, and its conductivity confirmed after drying by the addition of

electronic interconnects (**Figure 6C**). We demonstrated long-length light-emitting diode (LED) circuits by using the electrically conductive hydrogels where successful lighting of an LED was achieved with standard electrical wire. Based on these results, we expected that the bioprinting system with patternable conductive hydrogel would have several significant impacts on human health. Concretely, 3D printing a structure composed of conductive polymers can be useful in a wide variety of electrical applications, such as biological signal recording device, stimulation electrode, drug delivery device, neural differentiation culture system, and neural tissue regeneration [10, 19].

3.7 The influence of ES on neuronal differentiation capability of encapsulated neural cells

The 3D printed conductive hydrogel structure can effectively transfer ES through the bulk material as well as the scaffold surface. Therefore, it can be useful in a myriad of potential electrical applications. To illustrate one potential application, we prepared DRG cell-encapsulated GelMA hydrogels which were integrated with 3D printed conductive structure, and evaluated the efficiency of neural differentiation by ES treatment. ES treatment has been shown to enhance neuronal cell protein expression leading to the generation of highly induced neuron-like cells [38, 39]. For this purpose, square pore of conductive hydrogel structures was filled with DRG cell-encapsulated GelMA hydrogel and subsequently exposed to ES for the induction of neuronal differentiation after 24 hours of culture. Confocal images showed the neural differentiation of encapsulated DRG cells in four different biological environments (**Figure 7**). Within 24 hours of differentiation, all DRG cells expressed two different neuronal markers with TUJ1 and neurofilament. No definite differences were observed in both non-conductive hydrogel structures (PEDOT:PSS 0 %) after ES treatment. In contrast, conductive hydrogel structures (PEDOT:PSS 0.91 %) showed enhanced neuronal differentiation with a significant difference in neuronal gene expression with or without ES

treatment. However, conductive hydrogel structures appeared strongly stained fluorescence intensity due to non-specific binding. Therefore, the additional quantitative analysis is required since it is difficult to figure out which is better in a conductive hydrogel with or without ES treatment. For quantitative evaluation of neural differentiation, qPCR was performed to examine mRNA expression of each group using various neuronal gene markers including Brain-derived neurotrophic factor (BDNF), Neurotrophin-3 (NT-3), and erbB2 (**Figure 8**). It is well known that BDNF expressed in the DRG plays a neuromodulatory role for supporting neuronal development and inducing hyperalgesia [40]. NT-3 is a widely accepted and known marker involved in spinal cord regeneration and the regulation of sensory neuron outgrowth [41]. Also, erbB2 is known as one of the four members of the ErbB family which is involved in the development of neural crease cells and their derivatives [42, 43]. Therefore, owing to their specific role(s) in neural differentiation, these neuronal gene markers were quantified in the current study. All neuronal gene expression in the non-conductive hydrogel structures (only PEG hydrogel) showed no statistical difference with or without ES. In contrast, a significant increase in BDNF, NT-3 and erbB2 gene expression was observed in conductive hydrogel structures (PEG with PEDOT:PSS) with ES than those without ES. These results may indicate that the conductive hydrogel structure provides a desirable effects on due to the systematic transfer of ES toward encapsulated DRG cells leading to enhanced neuronal differentiation. With these advantages, 3D conductive hydrogel structure is promising highly effective neural culture system for neural tissue engineering.

4. Conclusion

In summary, we have successfully employed a 3D printing system leading to the fabrication of patternable conductive hydrogels for the systematic delivery of ES for enhanced neural differentiation. The conductive hydrogel was shown to significantly improve electrochemical properties with the driven current on their surface. This conductive hydrogel was shown to exhibit minimal cytotoxic effects when cultured in direct contact with DRG cells. In addition, 3D printing of conductive hydrogels produced well-integrated scaffolds with pre-designed geometry. The current study focused on the development of a bioprinting system consisting of a 3D printable conductive hydrogel used in combination with ES for enhanced neural cell differentiation. The 3D printed conductive hydrogel structure significantly improved neuronal differentiation with electrochemically driven. These findings suggest that the development of 3D conductive hydrogel structure can be useful for interfacial bioelectronics with biological stimulation in order to regulate and induce cell behavior. In addition, it can be useful in a wide variety of bioelectrical application, such as a biological signal recording device, a stimulation electrode, neural differentiation culture system, and neural tissue regeneration.

Acknowledgment

This work was supported by March of Dimes Foundation's Gene Discovery and Translational Research Grant.

References

[1] R. Balint, N.J. Cassidy, S.H. Cartmell, Electrical Stimulation: A Novel Tool for Tissue Engineering, Tissue Eng Part B-Re, 19 (2013) 48-57.
[2] L. Ghasemi-Mobarakeh, M.P. Prabhakaran, M. Morshed, M.H. Nasr-Esfahani, H. Baharvand, S. Kiani, S. Al-Deyab, S. Ramakrishna, Application of conductive polymers, scaffolds and electrical stimulation for nerve tissue engineering, J Tissue Eng Regen M, 5 (2011) E17-E35.
[3] K.A. Chang, J.W. Kim, J.A. Kim, S. Lee, S. Kim, W.H. Suh, H.S. Kim, S. Kwon, S.J. Kim, Y.H. Suh, Biphasic Electrical Currents Stimulation Promotes both Proliferation and Differentiation of Fetal Neural Stem Cells, Plos One, 6 (2011).
[4] M. Yamada, K. Tanemura, S. Okada, A. Iwanami, M. Nakamura, H. Mizuno, M. Ozawa, R. Ohyama-Goto, N. Kitamura, M. Kawano, K. Tan-Takeuchi, C. Ohtsuka, A. Miyawaki, A. Takashima, M. Ogawa, Y. Toyama, H. Okano, T. Kondo, Electrical stimulation modulates fate determination of differentiating embryonic stem cells, Stem Cells, 25 (2007) 562-570.
[5] J.F. Feng, J. Liu, X.Z. Zhang, L. Zhang, J.Y. Jiang, J. Nolta, M. Zhao, Guided Migration of Neural Stem Cells Derived from Human Embryonic Stem Cells by an Electric Field, Stem Cells, 30 (2012) 349-355.
[6] S.Y. Park, J. Park, S.H. Sim, M.G. Sung, K.S. Kim, B.H. Hong, S. Hong, Enhanced Differentiation of Human Neural Stem Cells into Neurons on Graphene, Advanced Materials, 23 (2011) H263-+.
[7] F. Pires, Q. Ferreira, C.A.V. Rodrigues, J. Morgado, F.C. Ferreira, Neural stem cell differentiation by electrical stimulation using a cross-linked PEDOT substrate: Expanding the use of biocompatible conjugated conductive polymers for neural tissue engineering, Bba-Gen Subjects, 1850 (2015) 1158-1168.
[8] O. Akhavan, E. Ghaderi, Differentiation of human neural stem cells into neural networks on graphene nanogrids, Journal of Materials Chemistry B, 1 (2013) 6291-6301.
[9] W. Zhu, T. Ye, S.J. Lee, H. Cui, S. Miao, X. Zhou, D. Shuai, L.G. Zhang, Enhanced neural stem cell functions in conductive annealed carbon nanofibrous scaffolds with electrical stimulation, Nanomedicine, 14 (2018) 2485-2494.
[10] G. Kaur, R. Adhikari, P. Cass, M. Bown, P. Gunatillake, Electrically conductive polymers and composites for biomedical applications, Rsc Adv, 5 (2015) 37553-37567.
[11] S. Nambiar, J.T.W. Yeow, Conductive polymer-based sensors for biomedical applications, Biosens Bioelectron, 26 (2011) 1825-1832.
[12] S.J. Lee, T. Esworthy, S. Stake, S. Miao, Y.Y. Zuo, B.T. Harris, L.G. Zhang, Advances in 3D Bioprinting for Neural Tissue Engineering, Advanced Biosystems, 2 (2018) 1700213.
[13] S. Choi, H. Lee, R. Ghaffari, T. Hyeon, D.H. Kim, Recent Advances in Flexible and Stretchable Bio-Electronic Devices Integrated with Nanomaterials, Advanced Materials, 28 (2016) 4203-4218.
[14] R. Ravichandran, S. Sundarrajan, J.R. Venugopal, S. Mukherjee, S. Ramakrishna, Applications of conducting polymers and their issues in biomedical engineering, J R Soc Interface, 7 (2010) S559-S579.
[15] H. Jo, M. Sim, S. Kim, S. Yang, Y. Yoo, J.-H. Park, T.H. Yoon, M.-G. Kim, J.Y. Lee, Electrically

conductive graphene/polyacrylamide hydrogels produced by mild chemical reduction for enhanced myoblast growth and differentiation, Acta biomaterialia, 48 (2017) 100-109.
[16] S. Yang, L. Jang, S. Kim, J. Yang, K. Yang, S.W. Cho, J.Y. Lee, Polypyrrole/alginate hybrid hydrogels: electrically conductive and soft biomaterials for human mesenchymal stem cell culture and potential neural tissue engineering applications, Macromolecular bioscience, 16 (2016) 1653-1661.
[17] S.J. Lee, W. Zhu, M. Nowicki, G. Lee, D.N. Heo, J. Kim, Y.Y. Zuo, L.G. Zhang, 3D printing nano conductive multi-walled carbon nanotube scaffolds for nerve regeneration, J Neural Eng, 15 (2018) 016018.
[18] A.E. Jakus, E.B. Secor, A.L. Rutz, S.W. Jordan, M.C. Hersam, R.N. Shah, Three-Dimensional Printing of High-Content Graphene Scaffolds for Electronic and Biomedical Applications, Acs Nano, 9 (2015) 4636-4648.
[19] R. Balint, N.J. Cassidy, S.H. Cartmell, Conductive polymers: Towards a smart biomaterial for tissue engineering, Acta Biomaterialia, 10 (2014) 2341-2353.
[20] R.A. Green, R.T. Hassarati, J.A. Goding, S. Baek, N.H. Lovell, P.J. Martens, L.A. Poole-Warren, Conductive Hydrogels: Mechanically Robust Hybrids for Use as Biomaterials, Macromolecular Bioscience, 12 (2012) 494-501.
[21] B.L. Guo, L. Glavas, A.C. Albertsson, Biodegradable and electrically conducting polymers for biomedical applications, Prog Polym Sci, 38 (2013) 1263-1286.
[22] R.A. Green, N.H. Lovell, G.G. Wallace, L.A. Poole-Warren, Conducting polymers for neural interfaces: Challenges in developing an effective long-term implant, Biomaterials, 29 (2008) 3393-3399.
[23] M. Irimia-Vladu, "Green" electronics: biodegradable and biocompatible materials and devices for sustainable future, Chemical Society Reviews, 43 (2014) 588-610.
[24] K. Sun, S.P. Zhang, P.C. Li, Y.J. Xia, X. Zhang, D.H. Du, F.H. Isikgor, J.Y. Ouyang, Review on application of PEDOTs and PEDOT: PSS in energy conversion and storage devices, J Mater Sci-Mater El, 26 (2015) 4438-4462.
[25] D.N. Heo, N. Acquah, J. Kim, S.J. Lee, N.J. Castro, L.G. Zhang, Directly Induced Neural Differentiation of Human Adipose-Derived Stem Cells Using Three-Dimensional Culture System of Conductive Microwell with Electrical Stimulation, Tissue Eng Part A, 24 (2018) 537-545.
[26] Y.Y. Lee, H.Y. Kang, S.H. Gwon, G.M. Choi, S.M. Lim, J.Y. Sun, Y.C. Joo, A Strain-Insensitive Stretchable Electronic Conductor: PEDOT:PSS/Acrylamide Organogels, Advanced Materials, 28 (2016) 1636-1643.
[27] N.J. Castro, J. O'Brien, L.G. Zhang, Integrating biologically inspired nanomaterials and table-top stereolithography for 3D printed biomimetic osteochondral scaffolds, Nanoscale, 7 (2015) 14010-14022.
[28] D.N. Heo, W.K. Ko, M.S. Bae, J.B. Lee, D.W. Lee, W. Byun, C.H. Lee, E.C. Kim, B.Y. Jung, I.K. Kwon, Enhanced bone regeneration with a gold nanoparticle-hydrogel complex, Journal of Materials Chemistry B, 2 (2014) 1584-1593.
[29] D.N. Heo, N.J. Castro, S.J. Lee, H. Noh, W. Zhu, L.G. Zhang, Enhanced bone tissue

regeneration using a 3D printed microstructure incorporated with a hybrid nano hydrogel, Nanoscale, 9 (2017) 5055-5062.

[30] S.H. Ouyang, Y.T. Xie, D.P. Wang, D.L. Zhu, X. Xu, T. Tan, H.H. Fong, Surface Patterning of PEDOT:PSS by Photolithography for Organic Electronic Devices, J Nanomater, DOI Artn 603148 10.1155/2015/603148(2015).

[31] S.H. Ouyang, Y.T. Xie, D.P. Wang, D.L. Zhu, X. Xu, T. Tan, J. DeFranco, H.H. Fong, Photolithographic Patterning of Highly Conductive PEDOT:PSS and Its Application in Organic Light-Emitting Diodes, J Polym Sci Pol Phys, 52 (2014) 1221-1226.

[32] B. Charlot, G. Sassine, A. Garraud, B. Sorli, A. Giani, P. Combette, Micropatterning PEDOT:PSS layers, Microsyst Technol, 19 (2013) 895-903.

[33] C. Yu, C. Wang, X. Liu, X. Jia, S. Naficy, K. Shu, M. Forsyth, G.G. Wallace, A Cytocompatible Robust Hybrid Conducting Polymer Hydrogel for Use in a Magnesium Battery, Adv Mater, 28 (2016) 9349-9355.

[34] J.Y. Oh, M. Shin, J.B. Lee, J.H. Ahn, H.K. Baik, U. Jeong, Effect of PEDOT Nanofibril Networks on the Conductivity, Flexibility, and Coatability of PEDOT:PSS Films, Acs Appl Mater Inter, 6 (2014) 6954-6961.

[35] J. Nevrela, M. Micjan, M. Novota, S. Kovacova, M. Pavuk, P. Juhasz, J. Kovac Jr, J. Jakabovic, M. Weis, Secondary doping in poly (3, 4-ethylenedioxythiophene): Poly (4-styrenesulfonate) thin films, Journal of Polymer Science Part B: Polymer Physics, 53 (2015) 1139-1146.

[36] N. Kim, S. Kee, S.H. Lee, B.H. Lee, Y.H. Kahng, Y.R. Jo, B.J. Kim, K. Lee, Highly Conductive PEDOT: PSS Nanofibrils Induced by Solution-Processed Crystallization, Advanced Materials, 26 (2014) 2268-2272.

[37] S.J. Lee, W. Zhu, L. Heyburn, M. Nowicki, B. Harris, L.G. Zhang, Development of Novel 3-D Printed Scaffolds With Core-Shell Nanoparticles for Nerve Regeneration, Ieee T Bio-Med Eng, 64 (2017) 408-418.

[38] G. Thrivikraman, G. Madras, B. Basu, Electrically driven intracellular and extracellular nanomanipulators evoke neurogenic/cardiomyogenic differentiation in human mesenchymal stem cells, Biomaterials, 77 (2016) 26-43.

[39] A. Kotwal, C.E. Schmidt, Electrical stimulation alters protein adsorption and nerve cell interactions with electrically conducting biomaterials, Biomaterials, 22 (2001) 1055-1064.

[40] Y.T. Lin, L.S. Ro, H.L. Wang, J.C. Chen, xi Up-regulation of dorsal root ganglia BDNF and trkB receptor in inflammatory pain: an in vivo and in vitro study, J Neuroinflamm, 8 (2011).

[41] X.Y. Wang, P.Y. Gu, S.W. Chen, W.W. Gao, H.L. Tian, X.H. Lu, W.M. Zheng, Q.C. Zhuge, W.X. Hu, Endogenous neurotrophin-3 promotes neuronal sprouting from dorsal root ganglia, Neural Regen Res, 10 (2015) 1865-1868.

[42] M.T. Woldeyesus, S. Britsch, D. Riethmacher, L. Xu, E. Sonnenberg-Riethmacher, F. Abou-Rebyeh, R. Harvey, P. Caroni, C. Birchmeier, Peripheral nervous system defects in erbB2 mutants following genetic rescue of heart development, Gene Dev, 13 (1999) 2538-2548.

[43] S. Mizobuchi, H. Kanzaki, H. Omiya, Y. Matsuoka, N. Obata, R. Kaku, H. Nakajima, M. Ouchida, K. Morita, Spinal nerve injury causes upregulation of ErbB2 and ErbB3 receptors in rat dorsal root

ganglia, J Pain Res, 6 (2013) 87-94.

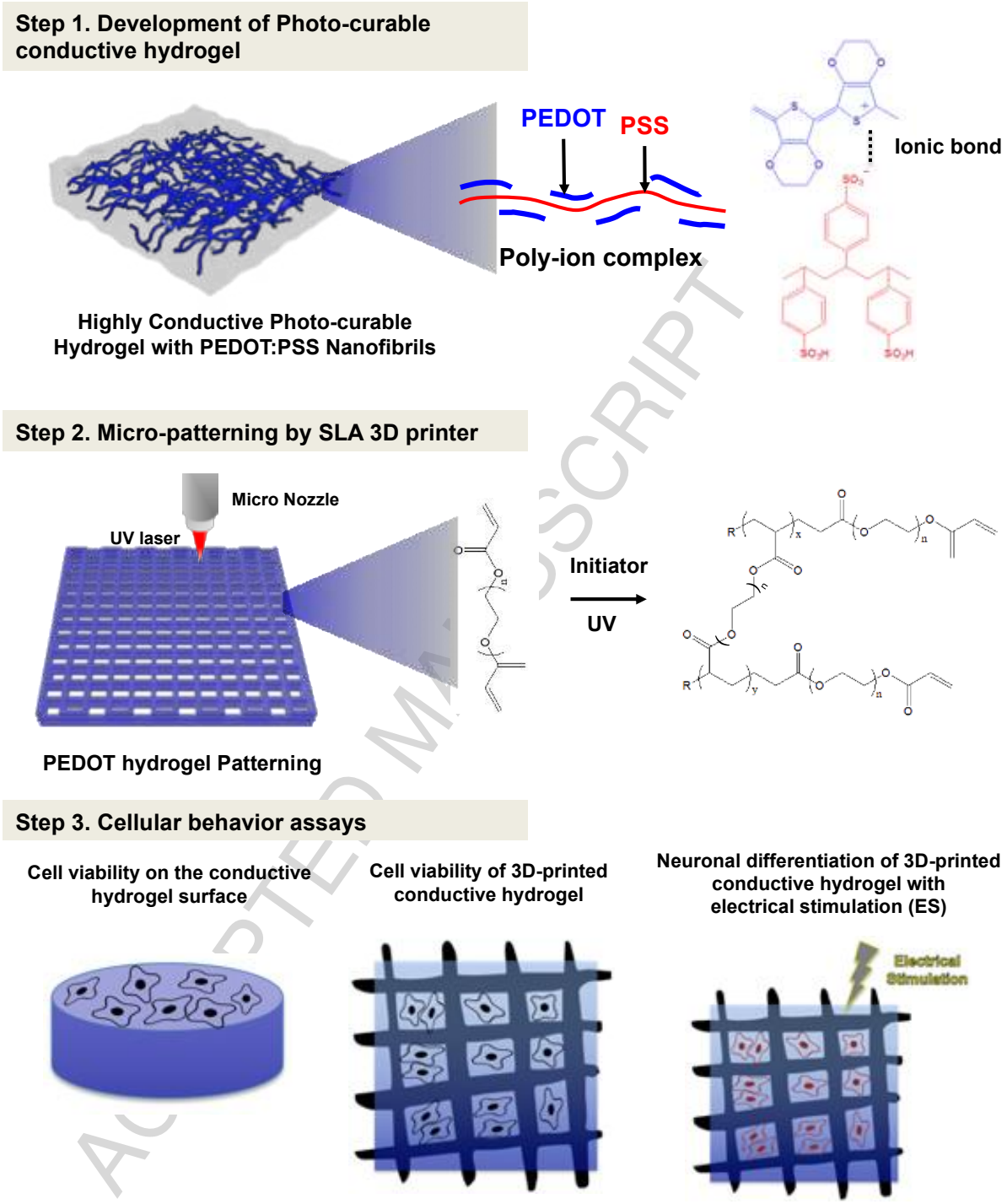

Figure 1. Schematic of the process to fabricate 3D conductive structure using SLA printing system and cellular behavior assays.

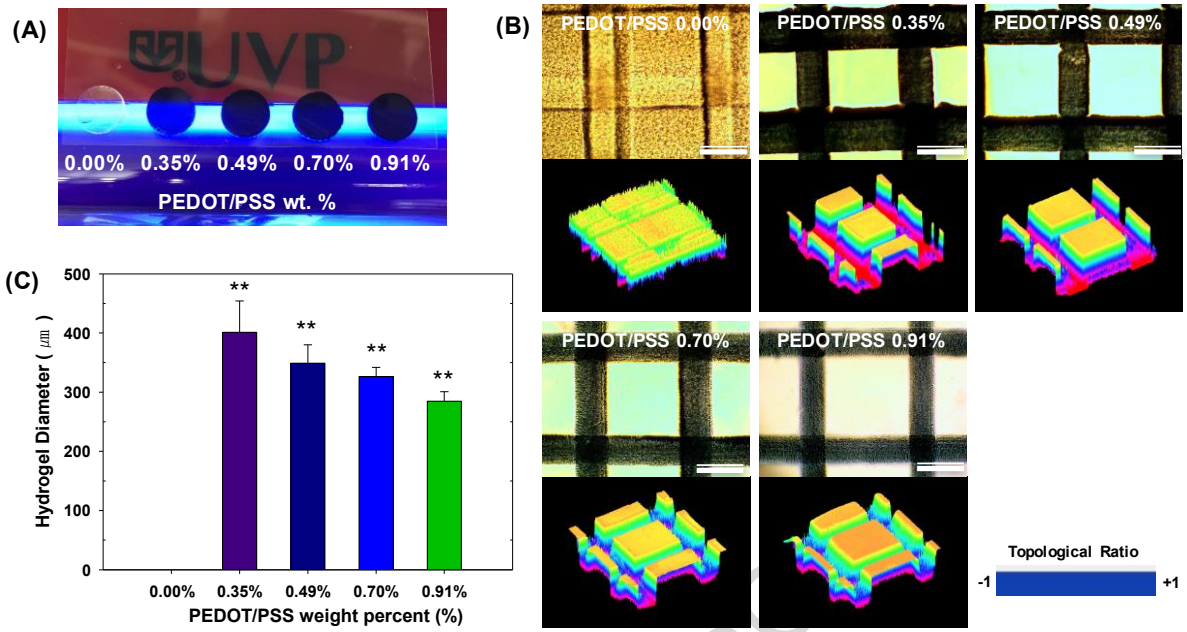

Figure 2. Fabrication of photocurable conductive hydrogels. (A) Optical images of conductive hydrogels with various concentrations of PEDOT/PSS 3D printing inks. (B) Optical and 3D surface plotting images, and (C) diameter of photo-patterned PEDOT/PSS hydrogels, scale bar = 500 μm (**$p < 0.01$).

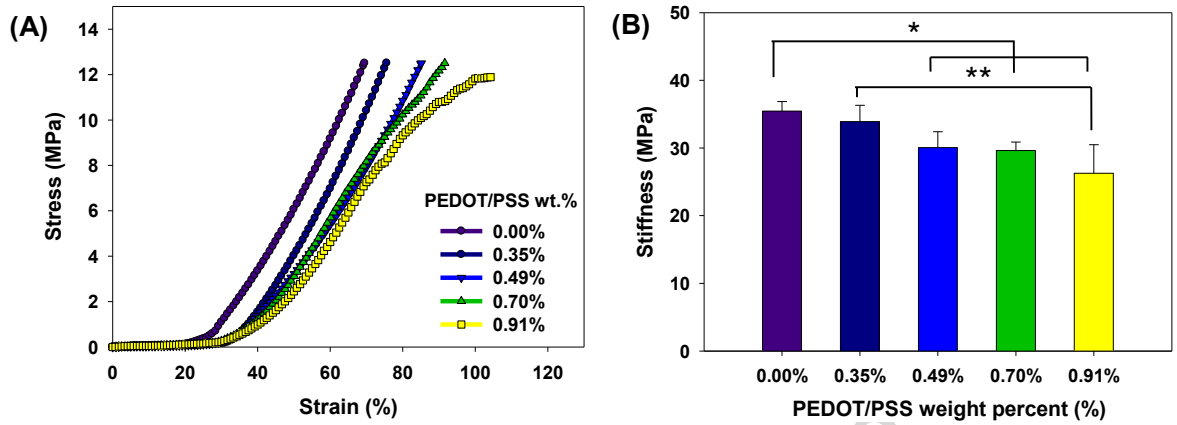

Figure 3. Mechanical properties of photocurable PEDOT/PSS hydrogels. (A) Compressive stress-strain curves of conductive hydrogels with various concentration of PEDOT/PSS, and (B) their stiffness (*p < 0.05 and **p < 0.01, n = 5).

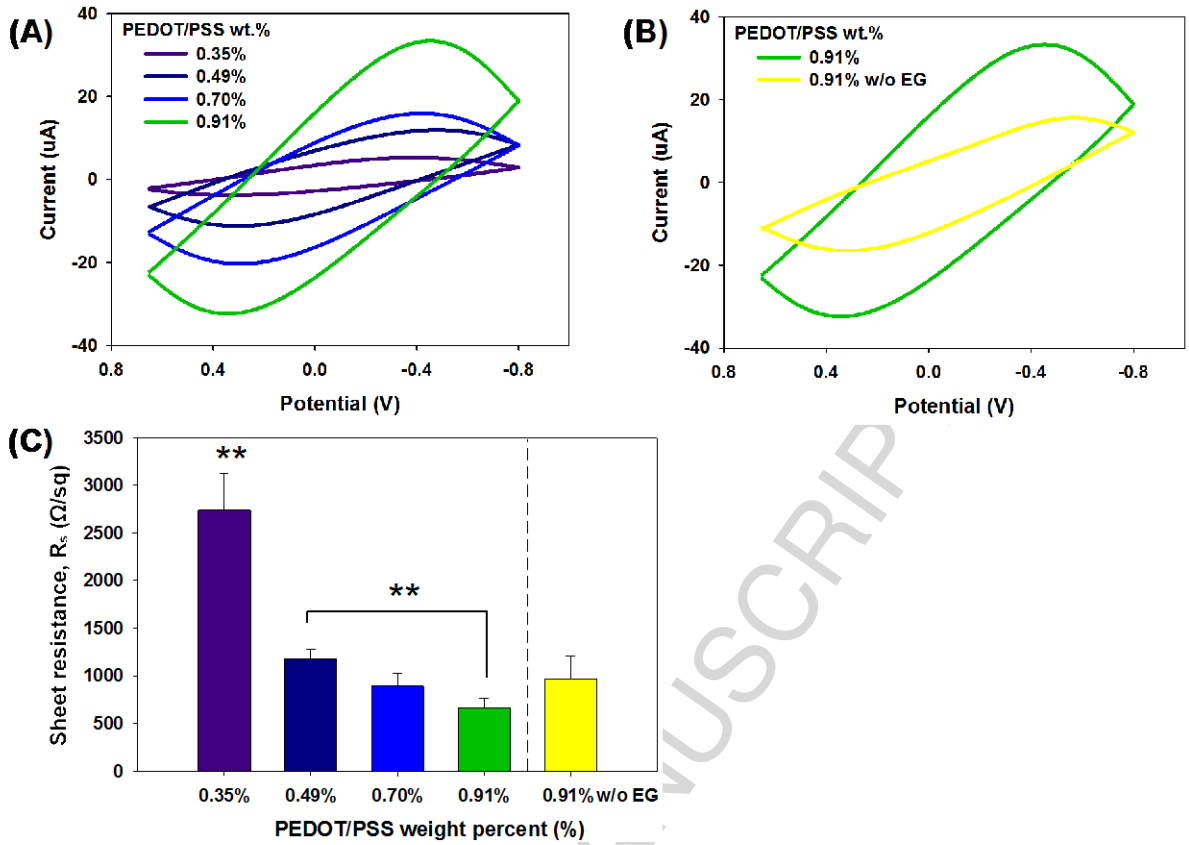

Figure 4. Electrochemical properties. (A, B) CV with scan range from -0.8 to 0.65 V at a scan rate of 100 mV/s. (C) Sheet resistance measured by a four-point probe ohmmeter (**p < 0.01, n = 5).

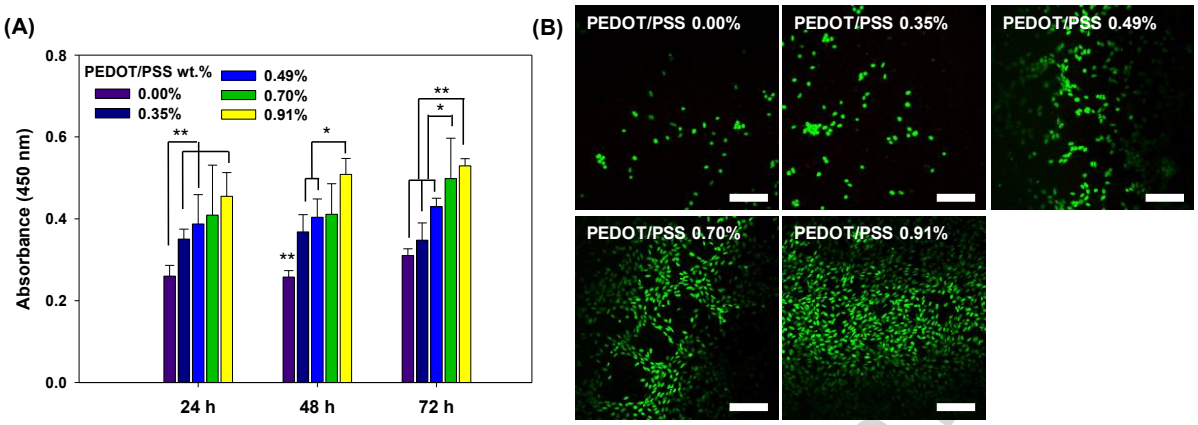

Figure 5. Proliferation and viability of dorsal root ganglion (DRG) cell culture on the PEDOT/PSS hydrogel surface, investigated by (A) CCK and (B) live/dead assay, scale bar = 100 µm (*$p < 0.05$ and **$p < 0.01$, n = 5).

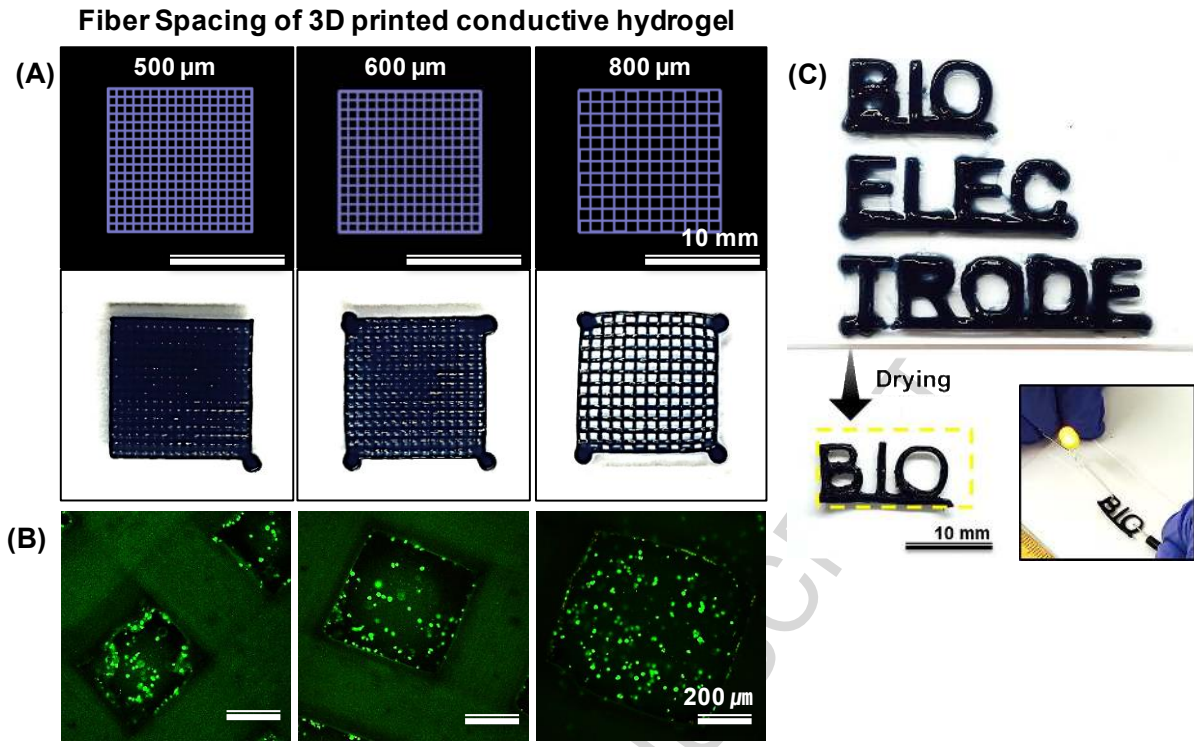

Figure 6. (A) Inputting AutoCAD patterns of parallel squares with the different width (width = 500, 600, and 800 μm) and the resulting patterns using photocurable PEDOT/PSS hydrogels. (B) Encapsulated DRG cells in GelMA with 3D printed PEDOT/PSS hydrogel on day 1 confirmed by a live/dead assay. (c) Optical images of PEDOT/PSS hydrogel in the swollen and dried states. Dried hydrogel was electrically connected` to an LED lamp.

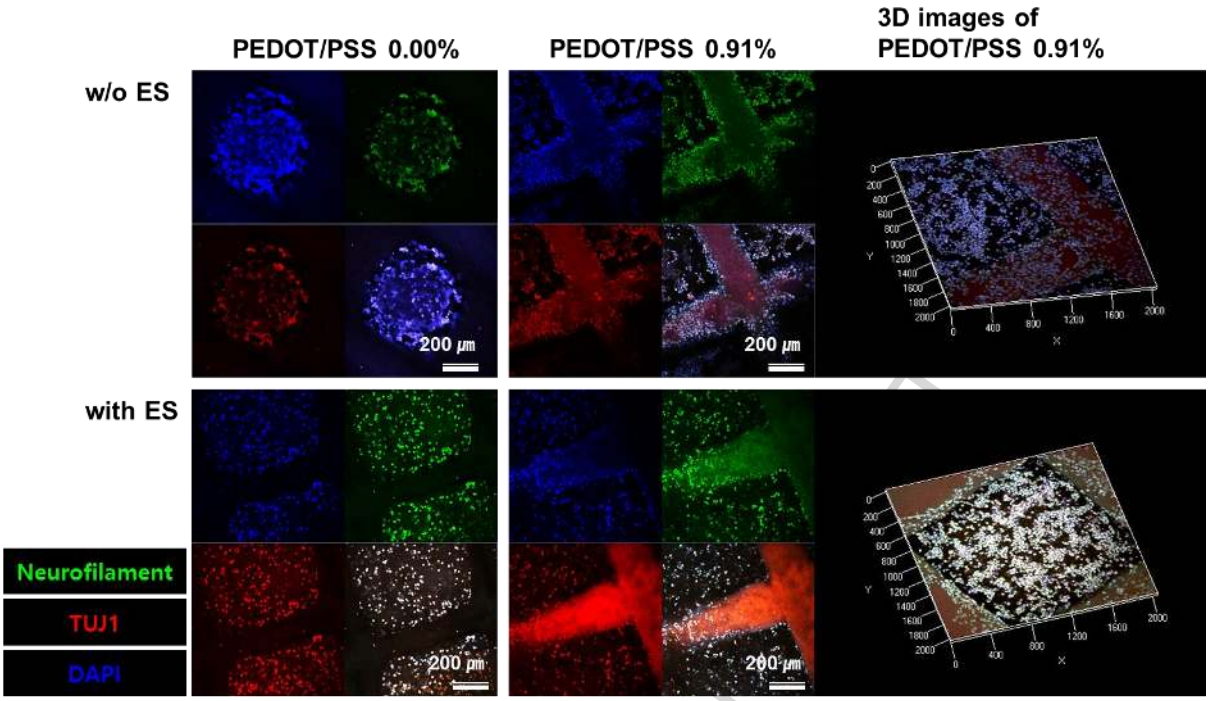

Figure 7. Immunofluorescence images of encapsulated DRG cells in GelMA with 3D printed PEDOT/PSS hydrogels, which were treated without or with ES for 2 days. Cells were stained with neurofilament (green), Tuj1 (red), and cell nuclei (blue).

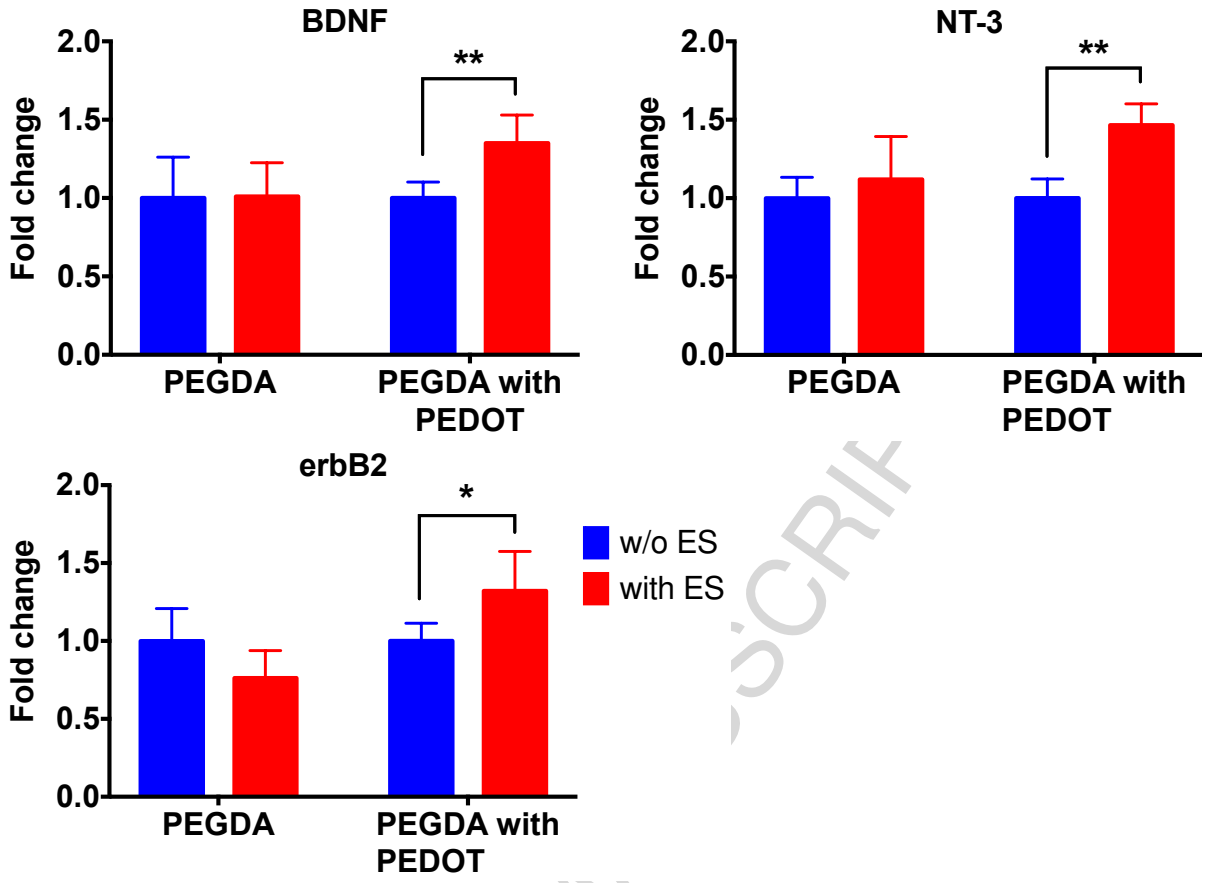

Figure 8. RT-PCR measurements for neural differentiation markers of encapsulated DRG cells in GelMA with 3D printed PEDOT/PSS hydrogels, which were treated without or with ES for 2 days. Relative gene expression of each gene (mean ± SD), normalized to the expression of the housekeeping gene GAPDH, are compared with each group without ES (*$p < 0.05$ and **$p < 0.01$, n = 5).

Highlights

- The presence of conductive polymer, PEDOT:PSS within printing material provides a conductive substrate.
- The conductive hydrogel structure significantly improved electrical potential with electrochemically driven current on the surface when compared to non-conductive hydrogel-based structure.
- 3D printed structure transmitted electrical stimulation to neuronal cells effectively induces neuronal differentiation.